PCCP

PAPER

DFT study of propane dehydrogenation on Pt catalyst: effects of step sites†

Ming-Lei Yang,[a] **Yi-An Zhu,**[a] **Chen Fan,**[a] **Zhi-Jun Sui,**[a] **De Chen**[b] **and Xing-Gui Zhou***[a]

Self-consistent periodic slab calculations based on gradient-corrected density functional theory (DFT-GGA) have been conducted to examine the reaction network of propane dehydrogenation over close-packed Pt(111) and stepped Pt(211) surfaces. Selective C–H or C–C bond cleaving is investigated to gain a better understanding of the catalyst site requirements for propane dehydrogenation. The energy barriers for the dehydrogenation of propane to form propylene are calculated to be in the region of 0.65–0.75 eV and 0.25–0.35 eV on flat and stepped surfaces, respectively. Likewise, the activation of the side reactions such as the deep dehydrogenation and cracking of C_3 derivatives depends strongly on the step density, arising from the much lower energy barriers on Pt(211). Taking the activation energy difference between propylene dehydrogenation and propylene desorption as the descriptor, we find that while step sites play a crucial role in the activation of propane dehydrogenation, the selectivity towards propylene is substantially lowered in the presence of the coordinatively unsaturated surface Pt atoms. As the sole C_3 derivative which prefers the cleavage of the C–C bond to the C–H bond breaking, propyne is suggested to be the starting point for the C–C bond breaking which eventually gives rise to the formation of ethane, methane and coke. These findings provide a rational interpretation of the recent experimental observations that smaller Pt particles containing more step sites are much more active but less selective than larger particles in propane dehydrogenation.

1. Introduction

In the past three decades, extensive efforts have been devoted to catalytic dehydrogenation of paraffin on transition metals for light olefin production.[1–3] Special interest has been focused on the catalysts for propane dehydrogenation to form propylene because propane is easily available and there is an increasing demand for propylene. Though several catalytic dehydrogenation techniques such as Oleflex, Catofin, *etc.* have been commercialized, there is still plenty of room to improve the catalyst performance for longer operation cycle and higher selectivity.

Pt and Pt-based alloys have long been known as important catalysts in hydrogenation of olefins, and the dehydrogenation and cracking of paraffins.[4–8] However, the major problem for Pt-based catalysts is the C–C cleavage of long-chain hydrocarbons, leading to coke formation.[9–20] As a result, the catalyst losses its activity quickly and must be regenerated cyclically, which increases the process complexity. In the propane dehydrogenation system, it is therefore of vital importance to understand the reaction mechanism so as to improve the selectivity towards propylene and suppress coke formation

The dehydrogenation of propane involves a series of side reactions, including deep dehydrogenation and hydrogenolysis of propane, and produces numerous fragments ranging from C_1 to C_3 species adsorbed on the catalyst surface. In order to understand the reaction mechanism involved in the dehydrogenation process, a large number of kinetic and spectroscopic measurements have been performed to identify the possible reactive intermediates on the catalyst.[1,21–28] In early 1982, Salmerón and Somorjai[29] showed that propylene was adsorbed readily on Pt(111) and remained stable with no chemical decomposition up to around 280 K. A detailed thermochemistry of C_3 metallacycles,[30] determined by temperature

[a] State Key Laboratory of Chemical Engineering, East China University of Science and Technology (ECUST), Shanghai 200237, China. E-mail: xgzhou@ecust.edu.cn; Fax: +86-21-64253528; Tel: +86-21-64253509
[b] Department of Chemical Engineering, Norwegian University of Science and Technology (NTNU), N-7491 Trondheim, Norway
† Electronic supplementary information (ESI) available: Optimized structures of all the possible adsorption configurations of C_3 species, as well as the binding energies; several possible TSs together with activation energies to confirm our results; the data set from Fig. 8. See DOI: 10.1039/c0cp00341g
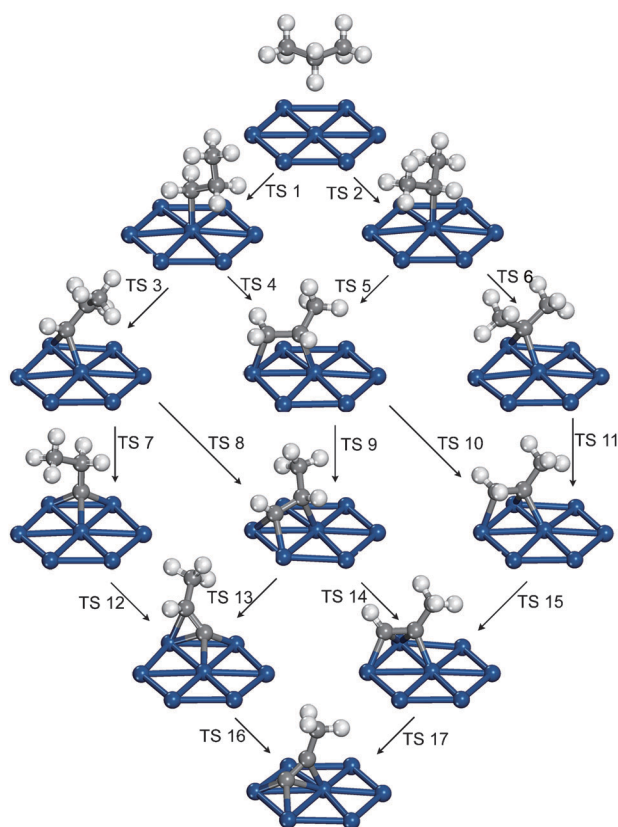
This journal is © the Owner Societies 2011

Phys. Chem. Chem. Phys., 2011, **13**, 3257–3267 | 3257

Fig. 1 Elementary steps involved in propane dehydrogenation. Carbon atoms are colored grey, hydrogen atoms white and Pt atoms blue.

programmed desorption (TPD) and reflection-absorption infrared spectroscopy (RAIRS), indicated that the allylic species was firstly hydrogenated to propylene and then decomposed to propylidyne (CCH_2CH_3) and eventually to H_2 and surface carbon. Based on the fluorescence yield near edge spectroscopy (FYNES) experiments, propyne was found to be adsorbed through the π system, with the methyl group orientated up from the Pt surface plane.[31] However, the adsorbed propyne was quite active. At room temperature, it was reported that propyne was converted to propylidyne in the presence of hydrogen on the catalyst surface.[32] The recent theoretical calculations were consistent with their experimental results.[30–36] Based on the Brønsted-Evans-Polanyi (BEP) relationship, the activation energy can be estimated from the reaction heat.[33,35] Valcárcel et al.[36] studied the thermodynamics of the dehydrogenation of propylene on Pt(111) through density functional theory (DFT) calculations. They proposed that the formation of propylidyne was the most exothermic step in the dehydrogenation process. It was therefore reasonable to assume that the barrier for the formation of propylidyne was lower than those for the other reactions. In addition, the subsequent dehydrogenation of propyl towards propylene was suggested to be the rate-determining step in propane dehydrogenation on the basis of the reported kinetic study.[27,28] However, no first-principles calculations are hitherto conducted to investigate the detailed reaction mechanism for propane dehydrogenation.

It has been long observed that the bond scission in hydrocarbon conversion reactions is generally aided by corrugated surfaces. Step sites showed much higher activity towards C–H bond and C–C bond cleavage than the flat surface.[37] For example, the *d*-band center of edge atoms is 0.15 eV higher in energy than that of the atoms on a flat Pd surface.[38] In the past decade, extensive studies have been focused on the dissociation of C_1 and C_2 hydrocarbons on metal surfaces.[38–43] Vang et al.[43] performed DFT calculations and found that the stepped Ni surface could significantly lower the barriers for ethylene dissociation, especially for the C–C bond breaking. To date, however, no general framework has been established for the surface structure effect on the selectivity towards propylene and coke formation in propane dehydrogenation. The experimental results regarding the effect of metal particle size are available from recent years.[5,44] Binder et al.[44] studied the turnover frequency (TOF) of Pd catalyst in ethylene hydrogenation and observed that a maximum TOF occurred for a Pd particle size of 3 nm. In the propane dehydrogenation system, smaller particles were found to be more active for propane conversion and coke formation while larger ones showed lower activity but higher selectivity towards propylene.[5] It is well known that as the particle size is increased, the population of the flat surface sites increases while that of the step sites decreases. It is therefore expected that the coke formation on Pt catalyst is mostly attributed to the C–C breaking on step sites.

In the present work, DFT calculations are employed to investigate the successive dehydrogenation and cracking of propane on Pt(111) and Pt(211). We focus on the dissociation of all the C_3 intermediates, and predict the possible products for the dehydrogenation and cracking from kinetic and thermodynamic points of view. The complex reaction network to be investigated is summarized in Fig. 1.

The paper is organized as follows. In section 2, details of the computational method are described, and in section 3, the activation energies and transition states for all the dehydrogenation and cracking steps on Pt(111) and Pt(211) are determined so as to reveal the reaction mechanism for propane dehydrogenation. In section 4, we conclude by discussing the effect of the surface structure on the catalytic activity and selectivity towards propylene. Finally, the reaction pathway for C–C bond breaking and the overall reaction scheme for propane dehydrogenation are elucidated.

2. Computational details

The plane-wave density functional theory calculations are carried out with the VASP package,[45–47] where Kohn–Sham equations are solved self-consistently with the generalized gradient approximation functional proposed by Perdew, Burke, and Ernzerhof.[48] The interactions between valence electrons and ion cores are represented by Blöchl's all-electron-like projector augmented wave method (PAW),[49] which regards the 6s 5d states as the valence configuration for Pt, 2s 2p states for C and 1s state for H. A plane wave energy cutoff of 400 eV is used in these calculations to achieve a tight convergence. Brillouin zone sampling is performed by using a Monkhorst–Pack grid with respect to the symmetry of
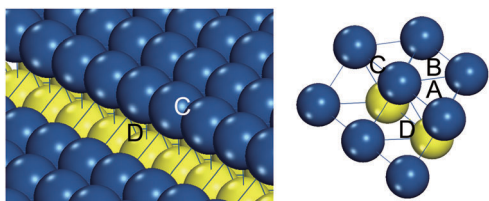
Fig. 2 Two side views of the stepped Pt(211) surface. The Pt atoms below the outermost layer are in yellow. (A) The near-edge-hcp site; (B) The fcc site; (C) The edge-bridge site; (D) The step-corner site. These notations are used throughout this paper.

the system and the electronic occupancies are determined according to a Methfessel-Paxton scheme[50] with an energy smearing of 0.2 eV.

A four-layer slab with a $p(3\times3)$ supercell is used to represent the Pt(111) surface, achieving the coverage of adsorbates of 1/9 ML (monolayers). The equilibrium Pt–Pt interatomic distance is calculated to be 2.82 Å. The successive slabs are separated by a vacuum region as thick as 12 Å in order to avoid periodic interactions. The Monkhorst–Pack k-points set contains seven k-points in the x- and y-direction and one k-point in the z-direction. The bottom two layers of the slab are kept fixed to their crystal lattice positions. When studying the reactions at steps, a (1×4) unit cell with 9 layers is used. The step sites on Pt(211) are shown schematically in Fig. 2. In these calculations, the bottom four layers are fixed. Monkhorst Pack mesh of $4\times2\times1$ k-points sampling in the surface Brillouin zone are used on the stepped surface. The ground-state atomic geometries of bulk and surfaces are obtained by minimizing the Hellman–Feynman forces with the conjugate-gradient algorithm until the total force on each ion is below 0.03 eV/Å.

To determine the reaction pathways, the dimer method implemented in VASP is used to climb up the potential energy surface from minimum to saddle points.[51–53] From the initial point, the dimer method is used to find the lowest curvature mode that leads to the saddle point. A force tolerance of 0.03 eV/Å is used in all the transition state searches. During the electronic optimization, the total energy and band structure energy are converged to an accuracy of 1×10^{-7} eV/atom so as to obtain accurate forces.

The adsorption energy (ΔE_{ads}) of an adsorbate (C_3H_x) is defined with respect to the gas-phase propane and the adsorbed H. The adsorption energy is calculated according to the following expression

$$\Delta E_{ads} = (E_{C_3H_x/surface} - E_{C_3H_8(g)} - E_{surface})$$
$$+ (8 - x)(E_{H/surface} - E_{surface}) \qquad (1)$$

where $E_{C_3H_8}$, E_H and $E_{surface}$ are DFT total energies of gas-phase propane, hydrogen and bare surface, respectively. A negative ΔE_{ads} corresponds to an energy gain process.

3. Results and discussion

3.1 Adsorption of propane and propylene on Pt(111) and Pt(211)

In recent years, the chemisorption of propane and propylene on Pt surface has been extensively studied both experimentally

and theoretically. Wang investigated the effects of a surface step on molecular propane adsorption on Pt(6 5 5) through molecular dynamics simulations and found that the favored zone for propane adsorption was near the step edge on the Pt surface, and the unfavorable zone was the top of the surface step on the upper terrace.[25] However, propane could not be adsorbed on the surface by binding with the Pt atoms, which resulted in low adsorption energy. As for propylene, it had a half-saturated double bond (C=C), and could therefore be readily adsorbed and decomposed on the Pt surface. Below the saturated coverage, di-σ mode adsorption was favored, while further dosing of propylene led to π mode adsorption. Valcárcel et al.[54] performed DFT calculations to study the chemisorption of propylene on Pt(111). It was reported that propylene was preferentially adsorbed at the bridge site in the di-σ mode, and the binding energy was higher than that in the π mode.

On the basis of the slab model, the chemisorption of propane is investigated on both Pt(111) and Pt(211). On Pt(111), propane is initially placed near the four high-symmetry adsorption sites, atop, bridge, fcc, and hcp. The total energies of the optimized configurations are very close, and the adsorption energies fall within the range of −0.02–0.06 eV. The molecular propane is repelled by the metal surface, drifting over the Pt surface, as shown in Fig. 3(a). On Pt(211), geometry optimization is performed by assigning propane at several adsorption sites near the step edge. It is found that propane cannot bind to the Pt atoms, and the adsorption energy is −0.04 eV. The above results show that propane is weakly physisorbed on both Pt(111) and Pt(211).

The LEED analysis[32] indicated that propylene could be adsorbed at the Pt surface in both the di-σ and π modes. In our calculations, the adsorption energy in the di-σ mode on Pt(111) is 0.27 eV higher than that in the π mode, which is consistent with the results of Zaera and Chrysostomou.[1,26] As shown in Fig. 3(b), propylene is preferentially adsorbed at the Bridge site by binding with two Pt atoms. The length of the C=C bond in the di-σ mode adsorption is elongated to 1.50 Å (1.36 Å in gaseous propylene), which is close to the C–C distance of propane (1.54 Å). This indicates that the C=C
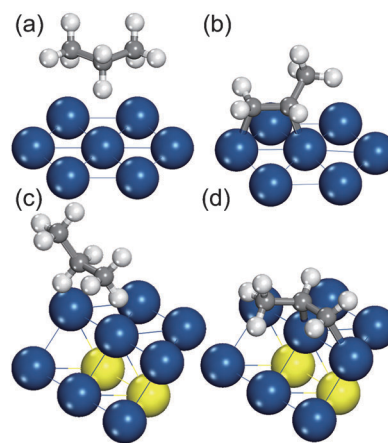

Fig. 3 Adsorption configurations of propane and propylene on both Pt(111) and Pt(211). (a) propane on Pt(111); (b) propylene on Pt(111); (c) propane on Pt(211); (d) propylene on Pt(211).

bond is weakened, due to the formation of covalent bonds between C and Pt atoms. On the stepped surface, propylene also favors the Bridge site on the step edge, and the optimized structure is similar to that on the flat surface. However, the adsorption energy is calculated to be −1.17 eV, 0.83 eV higher than that on the flat surface, indicating that binding to the less coordinated Pt atoms is preferred. It was reported that the adsorption of propylene could be weakened by increasing its coverage or in the presence of pre-adsorbed hydrogen atoms.[1] It is therefore an efficient way to promote propylene desorption by introducing coadsorbed hydrogen atoms on Pt surfaces.

3.2 Propane dehydrogenation to form propylene

The dehydrogenation process from propane to propylene involves at least two elementary steps. As for gaseous propane, it is known that the energy barrier for the C–H activation of methyl group is higher than that for the activation of methylene group (4.35 and 4.17 eV, respectively). In the catalytic system, propane dehydrogenation to produce propylene follows two steps: (i) the initial activation of propane occurs at both the methyl and methylene groups which generate 1-propyl and 2-propyl, respectively; (ii) propylene is formed via β-dehydrogenation of 1-propyl and 2-propyl. Each detached hydrogen atom requires an empty site for accommodation. It is therefore reasonable to expect that the coverage of hydrogen would significantly affect the dehydrogenation activation energy.

In step (i), the energy barriers for the initial activation of propane at both the methyl and methylene groups are calculated to be 0.69 and 0.70 eV on Pt(111), respectively. As shown in Fig. 4 (TS1 and TS2), propane is dehydrogenated over the top of a Pt atom, with the detached H atom positioned at the bridge site by elongating the C–H bond.

The remaining 1-propyl is located at the most stable atop site. The activated C–H bond in the transition state (TS) is stretched compared to the C–H bond length in the propane molecule (1.50 Å in the TS and 1.10 Å in propane molecule). As for the dehydrogenation taking place at the secondary C atom, the geometry of the transition state resembles the adsorption configuration of 2-propyl. The activation energy is only 0.01 eV higher than that for the dehydrogenation of methyl group, which indicates that there is no preference for the activation of C–H bonds. It is noted that these transition states are close to the final state on the potential energy surface, or in other words the TSs are "late".[37]

In step (ii), the activation energies for the dehydrogenation of 1-propyl and 2-propyl are calculated to be 0.70 and 0.68 eV, respectively. Likewise, the configurations of the transition states resemble the adsorption configuration of propylene. Both the two reactions take place at the bridge site, and the two activation energies are close and lower than 0.75 eV, which indicates that the dehydrogenation of both 1-propyl and 2-propyl is kinetically favorable to produce propylene. As shown in Table 1, the initial activation of propane is thermoneutral, while the subsequent dehydrogenation is an exothermic process.

For the conversion of propane to produce propylene on step sites, the same two reaction pathways are taken into account. The energy barriers for the initial activation of propane occurring at the methyl and methylene groups are calculated to be 0.32 and 0.28 eV, respectively. As shown in Fig. 5, both the two TSs (TS1 and TS2) resemble those on the flat surface. The subsequent dehydrogenation takes place at the edge-bridge site, and the energy barriers for the activation of 1-propyl and 2-propyl are 0.34 and 0.33 eV, respectively. In
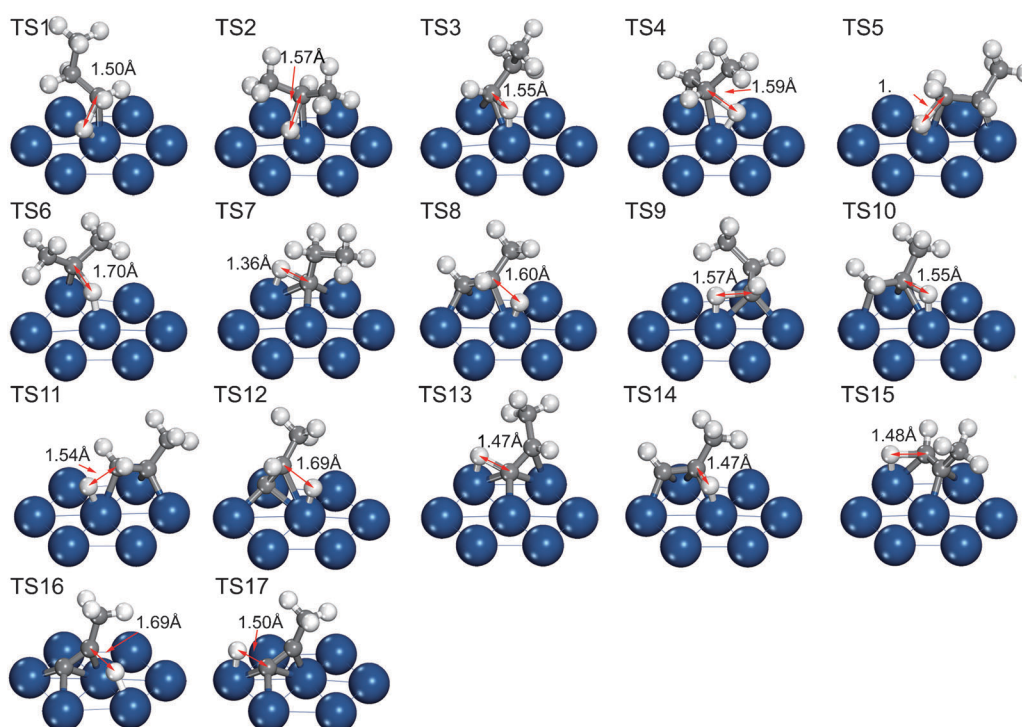

Fig. 4 Geometries of the transition states for propane dehydrogenation on Pt(111).

Table 1 Activation energies and reaction heats for the dehydrogenation of C_3 intermediates on Pt(111) and Pt(211)

	Surface reaction	ΔH (eV)		$\Delta E_{a,f}$ (eV)		$\Delta E_{a,r}$ (eV)	
		Pt(111)	Pt(211)	Pt(111)	Pt(211)	Pt(111)	Pt(211)
TS1	$CH_3CH_2CH_3* \rightarrow CH_3CH_2CH_2* + H*$	−0.07	−0.48	0.69	0.32	0.76	0.80
TS2	$CH_3CH_2CH_3* \rightarrow CH_3CHCH_3* + H*$	−0.06	−0.52	0.70	0.28	0.76	0.80
TS3	$CH_3CH_2CH_2* \rightarrow CH_3CH_2CH* + H*$	0.03	−0.53	0.73	0.17	0.70	0.70
TS4	$CH_3CH_2CH_2* \rightarrow CH_3CHCH_2* + H*$	−0.23	−0.65	0.70	0.34	0.93	0.99
TS5	$CH_3CHCH_3* \rightarrow CH_3CHCH_2* + H*$	−0.24	−0.61	0.68	0.33	0.92	0.94
TS6	$CH_3CHCH_3* \rightarrow CH_3CCH_3* + H*$	0.07	−0.56	0.84	0.23	0.77	0.79
TS7	$CH_3CH_2CH* \rightarrow CH_3CH_2C* + H*$	−0.79	−0.34	0.23	0.80	1.02	1.14
TS8	$CH_3CH_2CH* \rightarrow CH_3CHCH* + H*$	−0.19	−0.35	0.62	0.64	0.81	0.99
TS9	$CH_3CHCH_2* \rightarrow CH_3CHCH* + H*$	0.06	−0.23	0.76	0.44	0.70	0.67
TS10	$CH_3CHCH_2* \rightarrow CH_2CCH_2* + H*$	−0.01	−0.17	0.77	0.29	0.78	0.46
TS11	$CH_3CCH_3* \rightarrow CH_3CCH_2* + H*$	−0.33	−0.22	0.54	0.43	0.87	0.65
TS12	$CH_3CH_2C* \rightarrow CH_3CHC* + H*$	0.26	−0.06	1.04	0.83	0.78	0.89
TS13	$CH_3CHCH* \rightarrow CH_3CHC* + H*$	−0.33	−0.04	0.42	0.80	0.75	0.84
TS14	$CH_3CHCH* \rightarrow CH_2CCH* + H*$	−0.14	−0.21	0.76	0.76	0.90	0.97
TS15	$CH_3CCH_2* \rightarrow CH_3CCH* + H*$	−0.07	−0.27	0.77	0.61	0.84	0.88
TS16	$CH_3CHC* \rightarrow CH_3CC* + H*$	0.75	0.41	1.38	1.32	0.63	0.91
TS17	$CH_3CCH* \rightarrow CH_3CC* + H*$	0.56	0.58	1.39	1.50	0.83	0.92

the recent theoretical studies, similar energy barriers with values in the range of 0.29–0.42 eV for the initial activation of ethane to ethylene on Pt(110)-(1×2) were obtained by Anghel *et al.*[55,56]

3.3 Deep dehydrogenation on Pt(111) and Pt(211)

3.3.1 Dehydrogenation of propylene. In the propane dehydrogenation process, the deep dehydrogenation, especially the dehydrogenation of propylene, has a direct impact on the selectivity towards propylene. The dehydrogenation of methylene and methylidyne groups leads to 1-propenyl ($CHCHCH_3$) and 2-propenyl (CH_2CCH_3), respectively. In the following investigation of propylene dehydrogenation, the di-σ mode adsorption configuration of propylene is taken as the initial state. As shown in Fig. 4 (TS9), the methylene group is activated at the bridge site with the detached hydrogen relaxed to the atop site. The remaining 1-propenyl is located at the fcc site, adopting the most energetically
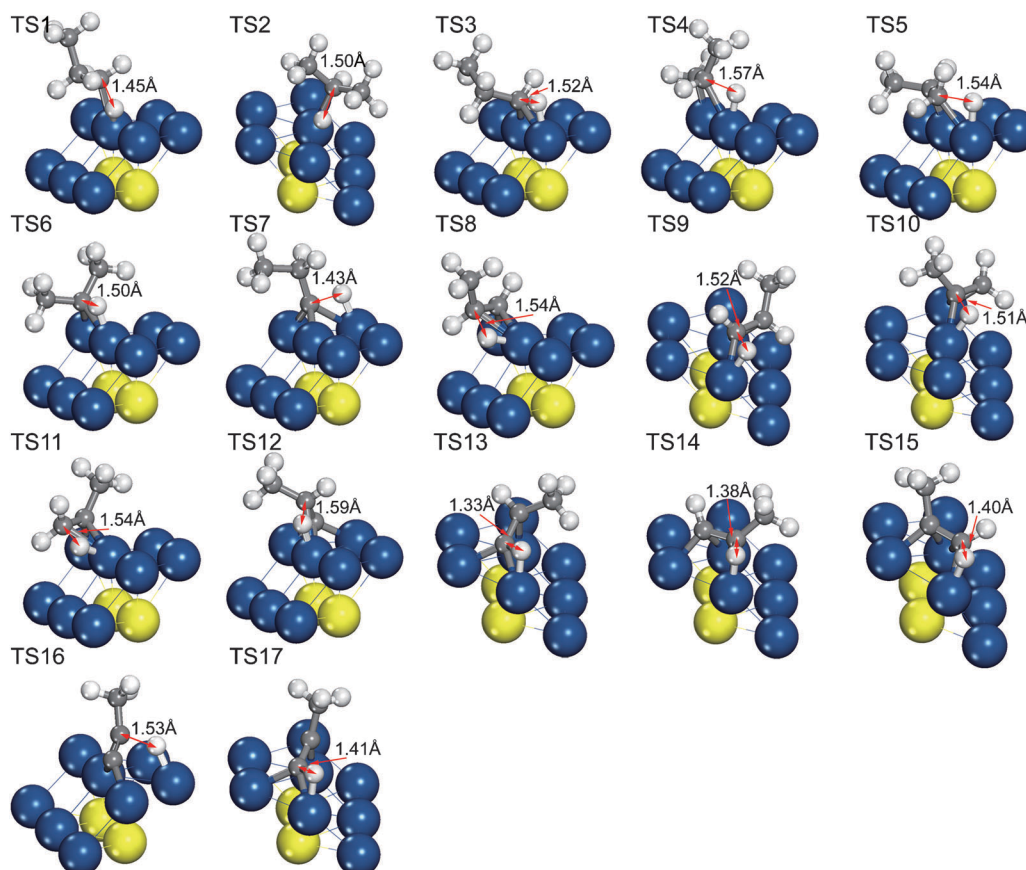

Fig. 5 Geometries of the transition states for propane dehydrogenation on Pt(211).

favorable adsorption configuration. The energy barrier is calculated to be 0.76 eV, and the final state is 0.06 eV higher in energy than the initial state, indicating the endothermic nature of the reaction. Experimentally, LEED analysis was used to verify that this reaction takes place by the capture of 1-propenyl.[32] As for the activation of the C–H bond at the middle carbon, a similar energy barrier of 0.77 eV is predicted. Using DFT calculations, Chen and Clachos[57] obtained an energy barrier of 0.84 eV for the dehydrogenation of ethylene on Pt(111), and Vang et al.[43] claimed a lower barrier of 0.68 eV on Ni(111).

On Pt(211), the energy barriers for propylene dehydrogenation are significantly lowered (the barriers for TS9 and TS10 are 0.29 and 0.44 eV, respectively). Meanwhile, the reverse reactions, namely the hydrogenation of propylene to produce 1-propyl and 2-propyl, are hindered by much higher energy barriers (0.99 eV to 1-propyl and 0.94 eV to 2-propyl, respectively), which indicates a remarkable preference of propylene to be further dehydrogenated. The geometries of the transition states (TS9 and TS10) are found to be different from those on the flat surface. As shown in Fig. 4, the activation of the C–H bond takes place at the edge-bridge site. Both the remaining 1-propenyl and 2-propenyl favor to bind with two Pt atoms to keep C sp[3]-hybridized.

3.3.2 Formation of propylidyne. Under ultra high vacuum conditions, propylene was observed to decompose to propylidyne just below room temperature.[22] The DFT study performed by Valcárcel et al.,[36] verified that propylidyne was the most energetically favorable intermediate on Pt(111). The formation of propylidyne from propane is likely to be achieved via two intermediates, namely 1-propyl and 1-propylidene (CHCH₂CH₃). The activation energy for the dehydrogenation of 1-propyl towards 1-propylidene is close to that for the initial activation of propane. 1-propylidene can be readily dehydrogenated to form propylidyne as long as the former is produced by

the α-dehydrogenation of 1-propyl. The corresponding activation energy is calculated to be only 0.23 eV, much lower than those for the other dehydrogenation reactions. As shown in Fig. 4 (TS7), the detached hydrogen is located at the atop site, and the remaining propylidyne is adsorbed at the most stable fcc site. The optimized length of the activated C–H bond is measured to be 1.36 Å, which is the shortest among all the TSs for dehydrogenation steps. It is difficult for propylidyne to be further dehydrogenated to form propenylidene (CCHCH₃) or hydrogenated to form 1-propylidene. These high energy barriers verify that propylidyne is the most stable C₃ species on the Pt(111) surface. However, the energy barrier for the propylidyne formation on step sites is 0.52 eV higher in energy than that on Pt(111). Chen and Vlachos[57] obtained similar energy barriers for the formation of ethylidyne (CCH₃), 0.28 and 0.86 eV on Pt(111) and Pt(211), respectively. Furthermore, it was shown by experiments that the coadsorption of hydrogen could inhibit the decomposition of ethylidyne on Pt(111).[58]

3.3.3 Formation of propynyl. Propynyl is the most energetically unfavorable species on the flat surface because the reaction heat from propane to propynyl is highest among all the C₃ derivatives.[36] Jacob and Goddard[59] have investigated the chemisorption of the C₂ species, and found that ethynyl was adsorbed on the surface with C sp²-hybridized. The heat formation analysis also indicated that ethynyl (CCH) was the most energetically unfavorable C₂ derivative. Propynyl can be formed by detaching one hydrogen atom from propenylidene or propyne. The activation energies are 1.38 eV for TS16 and 1.39 eV for TS17, which are much higher than those for the other dehydrogenation reactions. It is therefore expected that the end-point for the deep dehydrogenation process on Pt(111) is propyne and propenylidene.

On step sites, both propenylidene and propyne are predicted to be readily formed because of the low energy barriers and
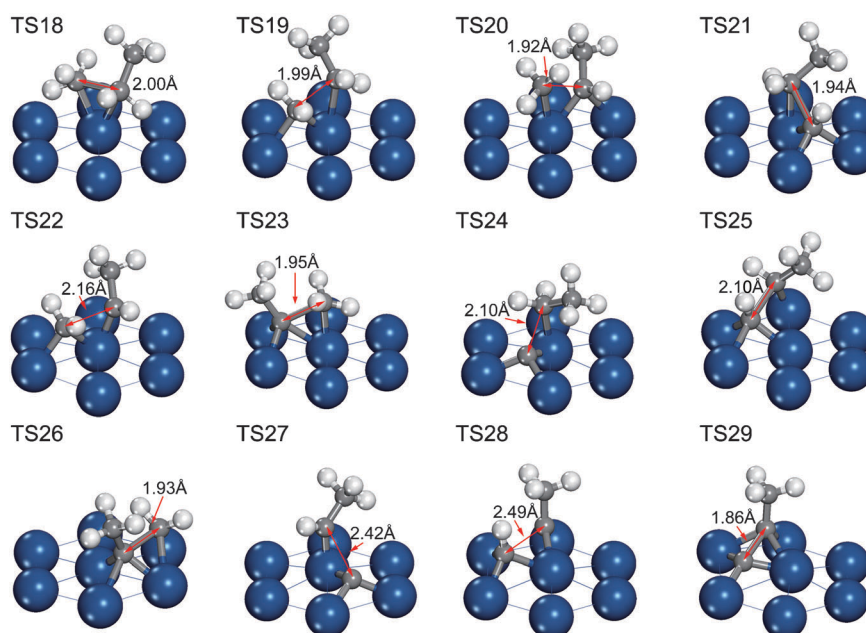

Fig. 6 Geometries of the transition states for C–C bond cleavage of C₃ intermediates on Pt(111).

3262 | *Phys. Chem. Chem. Phys.*, 2011, **13**, 3257–3267

This journal is © the Owner Societies 2011

strong binding strength. However, the activation of propyne and propenylidene to form propynyl is also inhibited on step sites because the energy barriers are predicted to be as high as 1.50 and 1.32 eV. As for the C_2 species, CHCH was also found to be formed at low surface coverages on Pt(110)-(1×2) at 300 K.[60]

3.4 C–C cleavage of C_3 intermediates on Pt(111) and Pt(211)

The bond energies of C–C, C=C and C≡C are calculated to be −3.95, −7.59 and −9.87 eV, indicating that the scission of these bonds is hindered by the high barriers in the gas phase.[61] In general, the C–C bond could be weakened if strong chemical bonds were formed between the metal and C atoms.[32,62] In the following study, the most preferred adsorption configurations are assigned to be the initial states for the C–C cleavage. According to the C_1 species involved in the products, the cracking reactions are classified into four categories, namely Type I for CH_3, Type II for CH_2, Type III for CH, and Type IV when there is no C_1 species. The geometries of the TSs for the cracking reactions on Pt(111) and Pt(211) are shown in Fig. 6 and Fig. 7, respectively. The activation energies and activated C–C bond lengths are listed in Table 2.

In Type I, three species are considered, namely $CH_3CH_2CH_3$, CH_3CHCH_3 and CH_3CCH_3. The C–C bond cleavage of propane is hindered by rather high barriers of 2.44 and 1.63 eV on Pt(111) and Pt(211), respectively. This is because propane is physisorbed on the Pt surface, and the interaction between the Pt atom and C–C bond is quite weak. The configurations of the transition states on the two surfaces are quite similar. As shown in Fig. 6 and Fig. 7 (TS18), the methyl and ethyl groups are located at the atop site and

repelled by each other, accompanied by the elongation of the C–C bond. For the other two cracking reactions, the methyl group is also located at the atop site, and the ethylidene ($CHCH_3$) and ethylidyne groups are located at the bridge and fcc sites, respectively, which is consistent with the work by Michealides and Hu.[34] The energy barriers for the three cracking steps on Pt(111), ranked in descending order, are as follows: $CH_3CH_2CH_3$ > CH_3CHCH_3 > CH_3CCH_3. Furthermore, in our recent work,[61] the binding energies of these species were −0.06 eV, −1.66 eV and −3.47 eV. Hence, it can be deduced that the removal of hydrogen can enhance the interaction between C and Pt atoms, and thus lower the barriers for the cracking steps.

In Type II, $CH_3CH_2CH_2$, CH_3CHCH_2 and CH_3CCH_2 are taken into account. The di-σ mode adsorption of propylene is assigned to be the initial state, and the energy barrier for the C–C bond breaking on Pt(211) is 0.58 eV lower than that on the flat surface, indicating that this reaction shows a strong preference for the step sites. The configuration of the transition state is apparently similar to the adsorption configuration of propylene in the π mode. Hence, propylene tends to firstly diffuse to the atop site, and then decomposed to methylene and ethylidene groups. With the low energy barrier for propylene dehydrogenation considered, propylene cracking is predicted to be unlikely to occur.

Type III includes the cracking of CH_3CH_2CH, CH_3CHCH and CH_3CCH. The energy barriers are dramatically lowered, as compared with those for Types I and II. For instance, the energy barrier for the cracking of 1-propylidene (1.18 eV) on Pt(111) is 0.51 eV lower than that for 1-propyl cracking (1.69 eV), and 1.31 eV lower than that for propane cracking. While the breaking of the C≡C bond in propyne is assumed
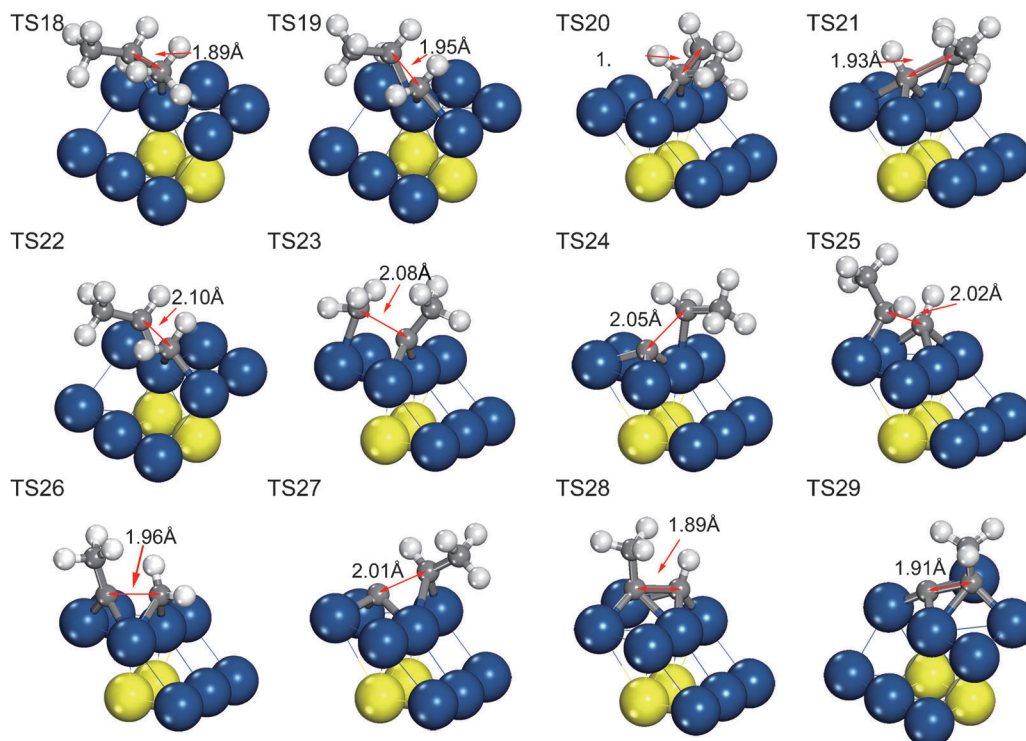

Fig. 7 Geometries of the transition states for C–C bond cleavage of C_3 intermediates on Pt(211).

Table 2 Activation energies for cracking of C_3 intermediates on Pt(111) and Pt(211)

	Surface reaction	ΔE_{act} (eV) Pt(111)	Pt(211)
TS18	$CH_3CH_2CH_3^* \rightarrow CH_3^* + CH_3CH_2^*$	2.44	1.63
TS19	$CH_3CH_2CH_2^* \rightarrow CH_2^* + CH_3CH_2^*$	1.69	1.12
TS20	$CH_3CHCH_3^* \rightarrow CH_3^* + CH_3CH^*$	1.81	1.22
TS21	$CH_3CH_2CH^* \rightarrow CH^* + CH_3CH_2^*$	1.18	1.50
TS22	$CH_3CHCH_2^* \rightarrow CH_2^* + CH_3CH^*$	2.00	1.42
TS23	$CH_3CCH_3^* \rightarrow CH_3^* + CH_3C^*$	1.31	1.73
TS24	$CH_3CH_2C^* \rightarrow C^* + CH_3CH_2^*$	1.91	1.67
TS25	$CH_3CHCH^* \rightarrow CH^* + CH_3CH^*$	1.59	2.15
TS26	$CH_3CCH_2^* \rightarrow CH_2^* + CH_3C^*$	1.62	1.49
TS27	$CH_3CHC^* \rightarrow C^* + CH_3CH^*$	2.19	2.00
TS28	$CH_3CCH^* \rightarrow CH^* + CH_3C^*$	0.86	1.39
TS29	$CH_3CC^* \rightarrow C^* + CH_3C^*$	0.96	0.97

to be quite difficult according to the aforementioned C≡C bond energies, the energy barrier for propyne cracking is lowest in Type III. As shown in the geometries of these three TSs, the methylidyne group is positioned at the most favored fcc site. The remaining ethyl and ethylidene groups prefer to bind with one Pt atom, and the ethylidyne group prefers three.

Type IV comprises the cracking of CH_3CH_2C, CH_3CHC and CH_3CC. The C–C bond breaking of propylidyne is hindered by an energy barrier of 1.91 eV, which indicates that this reaction is kinetically unfavorable on Pt(111). As for propynyl, while the barriers for the cleavage of the C–C bond are only about 1 eV on both surfaces, cracking is unlikely to occur because the formation of propynyl is hindered by high barriers for the dehydrogenation of propyne and propenylidene.

3.5 Thermodynamic factors in propane dehydrogenation

The reactions investigated in this work constitute a large amount of data for understanding the chemistry of dehydrogenated hydrocarbons on Pt surfaces. A linear Brønsted-Evans-Polanyi (BEP) relationship has been observed for the dissociation of gas-phase molecules such as CO_2, N_2 and O_2 across different metal surfaces.[63] However, for the cleavage of

different bonds over the same surface, it is not clear if the BEP relationship holds true. As shown in Fig. 8 (a), the plot of the energy barriers against the reaction heats for the bond-breaking steps on Pt(111) and Pt(211) does not give a straight line. Hence, the classical BEP relationship is not applicable in this case. In contrast, with the method suggested by Alcala et al.,[64] a good linear relationship was observed between the adsorption energies of final states (FSs) and TSs if the total energy of the gaseous reactant was taken as the energy reference. Two distinct regions have been identified in Fig. 8 (b). The upper region is dominated by the C–C bond-breaking steps while the bottom region is dominated by the C–H bond-breaking steps, and there is no obvious variation from Pt(111) to Pt(211). As proposed by Wang and Liu,[65] the energy barrier depended not only on thermodynamics, but also on the intrinsic bond polarity. The C–C and C–H bonds are known to possess different bond polarities. Under similar thermodynamic conditions, it is suggested that the C–H bond breaks first. As an example, both the breaking of C–C and C–H bonds of 1-propenyl on Pt(211) (Labeled as 1 and 2 in Fig. 8, respectively.) are almost thermoneutral, though the barrier height follows C–C > C–H.

3.6 Step effect on the catalytic activity towards propane dehydrogenation

The detailed one-dimensional potential energy diagrams for propane dehydrogenation on both the flat and stepped surfaces are shown in Fig. 9 and Fig. 10. The sum of the total energies of gas-phase propane and bare Pt surface is taken as the energy reference. It is assumed that any H atoms detached from the hydrocarbons are adsorbed on the surface at distances far away from the C_3 intermediates, which allows us to neglect the coadsorption effect of H.

As compared to the activation energies on the flat surface, the energy barriers for the dehydrogenation steps on the stepped surface are quite low, ranging from 0.28 to 0.34 eV, indicating the higher catalytic activity of the step sites. By DFT calculations, Liu and Hu have proposed the similar trend that the energy barrier for the activation of methane was
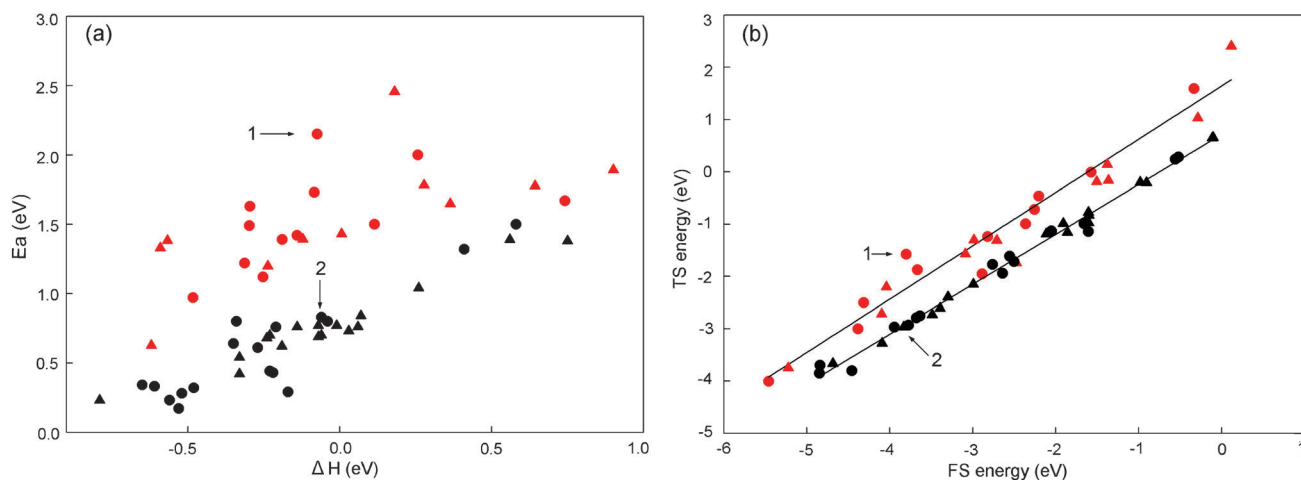

Fig. 8 (a) Plot of the energy barrier (E_a) against the reaction heat (ΔH). (b) Plot of the transition state (TS) adsorption energy against the final state (FS) adsorption energy for all the bond-breaking reactions on Pt(111) (triangles) and Pt(211) (circles). The red and black symbols denote the C–C and C–H bond-breaking reactions, respectively.

reduced by 0.3 eV on step sites compared to that on flat surfaces.[37] According to the Arrhenius equation, it can be estimated that a variation of 0.40 eV in the activation energy (e.g., the dehydrogenation of propane to form 2-propyl goes from the flat to stepped surface) will change the rate constant by 200 times. Thus, the stepped surface is kinetically more favorable for propane dehydrogenation.

3.7 Step effect on the selectivity towards propylene

In propane dehydrogenation, the deep dehydrogenation and cracking of C_3 derivatives, which eventually results in the formation of undesirable side products, will significantly lower the selectivity towards propylene production. As shown in Fig. 9 and Fig. 10, the C–C bond scission of propylene is hindered, arising from the much higher energy barriers than those for propylene dehydrogenation on both surfaces, which enables us to disregard the possibility of propylene cracking. In this sense, it is of great importance to elucidate the competition between propylene dehydrogenation and desorption. Here, the activation energy difference ($E_{deh} - E_{des}$) between the dehydrogenation and desorption of propylene is defined as the selectivity descriptor. In our calculations, the energy barrier for propylene desorption on the stepped surface is predicted to be 1.43 eV while the energy barrier for propylene dehydrogenation is only 0.29 eV. The negative selectivity descriptor indicates that the deep-dehydrogenated products, such as propenyl, propyne etc., are likely to be dominant on the stepped surface. That is, the selectivity towards propylene is substantially lowered in the presence of coordinatively unsaturated surface Pt atoms. However, on the close-packed Pt(111) surface, the energy barrier for propylene dehydrogenation is comparable to that for propylene desorption. Furthermore, it is reasonable to expect that the introduction of coadsorbed H atoms may increase the activation energy for propylene dehydrogenation and simultaneously promote the desorption of propylene under realistic experimental conditions. Therefore, while the catalytic activity of the flat surface toward propane dehydrogenation is lower than that on the stepped surface, the high selectivity towards propylene is attained on Pt(111).
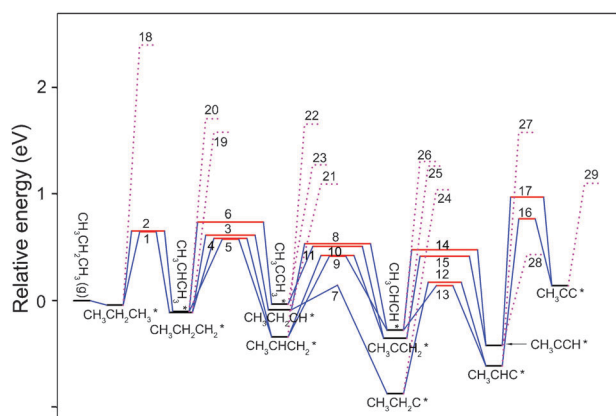

Fig. 9 Energy profile for propane dehydrogenation on Pt(111) including both the dehydrogenation steps (the solid lines) and the C–C cracking steps (the dotted lines).

3.8 Reaction pathway for C–C cleavage

In the dehydrogenation of propane, the key factor that affects the catalytic activity of Pt catalyst is coke formation.[67] Recent studies revealed that the coke on Pt surfaces was derived from the cracking of deep-dehydrogenated intermediates.[68,69] Hence, searching for the starting point for the C–C bond breaking is of crucial importance to describe the coke mechanism on Pt surfaces.

As for the step effect on the cracking reactions, it is apparent from Fig. 9 and Fig. 10 that most of the activation energies on the stepped surface are lower than those on the flat surface. Rioux et al.[66] reported the particle size effect on the hydrogenolysis of ethane over Pt catalyst. The TOF for ethane hydrogenolysis changes from 0.52 to 1.36×10^{-2} s^{-1} at 643 K for Pt particle size decreasing from 7.1 to 1.7 nm. Consequently, the presence of the stepped surface can promote not only the C–H bond-breaking steps but also the breaking of the C–C bonds.

In addition, the energy barriers for the C–C bond breaking are lowered more significantly than those for the dehydrogenation steps with the reactions moving from the flat to stepped surface. For instance, the energy barrier for the C–C bond breaking of propylene on Pt(211) is 0.58 eV lower than that on Pt(111), while the energy barrier for propylene dehydrogenation (TS9) on Pt(211) is only 0.32 eV lower.

As shown in Fig. 9 and Fig. 10, the energy barriers for the cracking of propane, 1-propyl, 2-propyl and propylene are significantly higher than those for the respective dehydrogenation steps on both Pt(111) and Pt(211), which indicates that the C–C bond breaking is not favored in the dehydrogenation of propane to produce propylene.

With the progression of the successive deep dehydrogenation, the activation energy differences between the cracking and dehydrogenation elementary steps are substantially reduced on both surfaces. It is therefore reasonable to suggest that the cleaving of the C–C bond may take place as the C_3 intermediates are deep dehydrogenated. Among the subsequent C_3 derivatives, propyne is the sole species which prefers the cleaving of the C–C bond to the C–H bond breaking [the activation energies for propyne cracking are 0.48 and 0.11 eV lower than those for propyne dehydrogenation on Pt(111) and Pt(211)]. Hence, propyne is suggested to be the starting point for the C–C bond cleaving which gives rise to the formation of C_1 and C_2 species as well as coke.

3.9 Overall reaction scheme for propane dehydrogenation

According to the experimental data, the C_3H_8 conversion and coke formation decreased quickly in the first tens of minutes on stream and then reached a steady state.[5] Thus, the process of propane dehydrogenation can be divided into two stages, namely the quick deactivation stage and the steady state. At the quick deactivation stage, the stepped surface is suggested to be the active center for all the reactions including the dehydrogenation and cracking steps, arising from the much lower energy barriers. The high catalytic activity of step sites provides a rational interpretation of the recent experimental observations that the TOF for small particles containing more stepped surfaces was much higher than that for larger particles
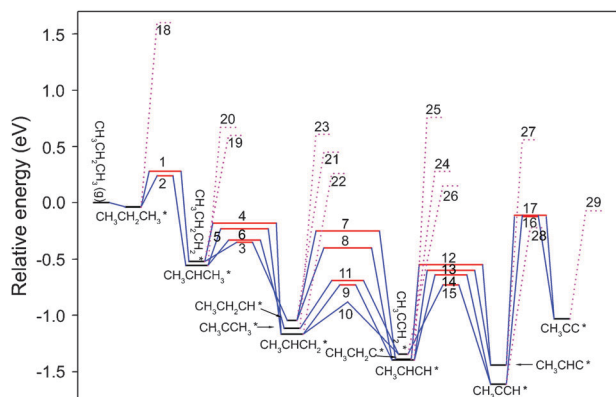
Fig. 10 Energy profile for propane dehydrogenation on Pt(211) including both the dehydrogenation steps (the solid lines) and the C–C cracking steps (the dotted lines).

at the quick deactivation stage.[5] However, the selectivity towards propylene on step sites is rather low because propylene prefers dehydrogenation to desorption, leading to the deep dehydrogenation of the subsequent C_3 derivatives. According to our calculations, the deep dehydrogenation process is terminated by propyne because the activation energy for propyne dehydrogenation is much higher than that for propyne cracking. Then, the C–C cleaving takes place and eventually leads to the formation of ethane, methane and coke.

As evidenced by the recent DFT work, step sites are suggested to be the active center for coke formation.[70] It is therefore reasonable to expect that the stepped surface loses the catalytic activity with the step sites blocked by the coke derived from the cracking reactions. At the steady state, the active center is transferred from the stepped to flat surface. As a result, the conversion of propane reduces to a large extent. Simultaneously, the selectivity toward propylene increases because the energy barrier for propylene desorption on the flat surface is substantially lowered compared with that on the stepped surface. Our calculation results indicate that the activation energy for propylene dehydrogenation is slightly lower than that for propylene desorption on Pt(111). However, under realistic experimental conditions, H atoms are coadsorbed with propylene, which can weaken the chemisorption of propylene and simultaneously promote the desorption of propylene.[1] Consequently, a higher selectivity towards propylene is expected on the flat surface.

4. Conclusion

This paper presents the first comprehensive DFT calculations to elucidate the reaction mechanism of propane dehydrogenation over Pt catalyst. The following conclusions regarding the effect of step sites on the catalytic reactivity towards propane dehydrogenation and the selectivity towards propylene have been obtained.

1. The energy barriers for the dehydrogenation of propane to form propylene are calculated to be in the region of 0.65–0.75 eV and 0.25–0.35 eV on the flat and stepped surfaces, respectively. The stepped surface is therefore kinetically more favorable for propane dehydrogenation.

2. Taking the activation energy difference between propylene dehydrogenation and propylene desorption as the selectivity descriptor, we find that while step sites play a crucial role in the activation of propane dehydrogenation, the selectivity towards propylene is substantially lowered in the presence of the coordinatively unsaturated surface Pt atoms.

3. As the sole C_3 derivative which prefers the cleaving of the C–C bond to the C–H bond breaking, propyne is suggested to be the starting point for the C–C bond breaking which eventually gives rise to the formation of methane, ethane and coke.

4. According to previous experimental work and our DFT calculations, the propane dehydrogenation process can be divided into two stages, namely the quick deactivation stage and steady state. At the quick deactivation stage, the stepped surface is suggested to be the active center for all the reactions including the dehydrogenation and cracking of C_3 derivatives. At this stage, the selectivity towards propylene is rather low because propylene prefers dehydrogenation to desorption. With the progression of the deep dehydrogenation and cracking of C_3 derivatives, coke is preferentially formed on the stepped surface. Then, the active center is transferred from the stepped to flat surface. At the steady state, while the catalytic activity towards propylene dehydrogenation is lowered, high selectivity towards propylene is attained because propylene desorption is promoted and simultaneously the deep dehydrogenation of propylene is suppressed on the flat surface. These findings provide a rational interpretation of the recent experimental observations that smaller Pt particles containing more step sites are much more active but less selective than larger particles in propane dehydrogenation.

Acknowledgements

References

1 F. Zaera and D. Chrysostomou, *Surf. Sci.*, 2000, **457**, 89.
2 S. B. Kogan and M. Herskowitz, *Catal. Commun.*, 2001, **2**, 179.
3 M. P. Lobera, C. Tellez, J. Herguido and M. Menendez, *Appl. Catal., A*, 2008, **349**, 156.
4 C. L. Yu, Q. J. Ge, H. Y. Xu and W. Z. Li, *Appl. Catal., A*, 2006, **315**, 58.
5 M. S. Kumar, D. Chen, J. C. Walmsley and A. Holmen, *Catal. Commun.*, 2008, **9**, 747.
6 P. Andy and M. E. Davis, *Ind. Eng. Chem. Res.*, 2004, **43**, 2922.
7 S. B. Kogan, H. Schramm and M. Herskowitz, *Appl. Catal., A*, 2001, **208**, 185.
8 N. Martin, M. Viniegra, E. Lima and G. Espinosa, *Ind. Eng. Chem. Res.*, 2004, **43**, 1206.
9 F. Cabrera, D. Ardissone and O. F. Gorriz, *Catal. Today*, 2008, **133**, 800.
10 Y. J. Tu and Y. W. Chen, *Ind. Eng. Chem. Res.*, 1998, **37**, 2618.
11 L. Y. Bai, Y. M. Zhou, Y. W. Zhang, H. Liu and M. H. Tang, *Catal. Lett.*, 2009, **129**, 449.
12 C. P. Poole and D. S. MacIver, *Adv. Catal.*, 1967, **17**, 223.

13 Y. W. Zhang, Y. M. Zhou, A. D. Qiu, Y. Wang, Y. Xu and P. C. Wu, *Catal. Commun.*, 2006, **7**, 860.
14 O. A. Bariås, A. Holmen and E. A. Blekkan, *J. Catal.*, 1996, **158**, 1.
15 L. H. Huang, B. L. Xu, L. L. Yang and Y. N. Fan, *Catal. Commun.*, 2008, **9**, 2593.
16 V. I. Hart, M. B. Bryant, L. G. Butler, X. Wu and K. M. Dooley, *Catal. Lett.*, 1998, **53**, 111.
17 G. J. Siri, G. R. Bertolini, M. L. Casella and O. A. Ferretti, *Mater. Lett.*, 2005, **59**, 2319.
18 Z. S. Nawaz, X. P. Tang, Q. Zhang, D. Z. Wang and W. Fei, *Catal. Commun.*, 2009, **10**, 1925.
19 J. M. Hill, R. D. Cortright and J. A. Dumesic, *Appl. Catal., A*, 1998, **168**, 9.
20 G. J. Siri, M. L. Casella, G. F. Santori and O. A. Ferretti, *Ind. Eng. Chem. Res.*, 1997, **36**, 4821.
21 D. Chrysostomou, C. French and F. Zaera, *Catal. Lett.*, 2000, **69**, 117.
22 P. S. Cremer, X. Su, Y. R. Shen and G. A. Somorjai, *J. Phys. Chem.*, 1996, **100**, 16302.
23 C. L. Kao and R. J. Madix, *J. Phys. Chem. B*, 2002, **106**, 8248.
24 Y. L. Tsai, C. Xu and B. E. Koel, *Surf. Sci.*, 1997, **385**, 37.
25 J. C. Wang, *Surf. Sci.*, 2003, **540**, 326.
26 F. Zaera and D. Chrysostomou, *Surf. Sci.*, 2000, **457**, 71.
27 I. Suzuki and Y. Kaneko, *J. Catal.*, 1977, **47**, 239.
28 P. Biloen, F. M. Dautzenberg and W. M. H. Sachtler, *J. Catal.*, 1977, **50**, 77.
29 M. Salmerón and G. A. Somorjai, *J. Phys. Chem.*, 1982, **86**, 341.
30 D. Chrysostomou, A. Chou and F. Zaera, *J. Phys. Chem. B*, 2001, **105**, 5968.
31 D. J. Burnett, A. M. Gabelnick, A. L. Marsh, D. A. Fischer and J. L. Gland, *Surf. Sci.*, 2004, **553**, 1.
32 R. J. Koestner, J. C. Frost, P. C. Stair, M. A. V. Hove and G. A. Somorjai, *Surf. Sci.*, 1982, **116**, 85.
33 O. R. Inderwildi, D. Lebiedz and J. Warnatz, *Phys. Chem. Chem. Phys.*, 2005, **7**, 2552.
34 A. Michaelides and P. Hu, *J. Am. Chem. Soc.*, 2000, **122**, 9866.
35 A. Michaelides, Z. P. Liu, C. J. Zhang, A. Alavi, D. A. King and P. Hu, *J. Am. Chem. Soc.*, 2003, **125**, 3704.
36 A. Valcárcel, J. M. Ricart, A. Clotet, F. Ilas, A. Markovits and C. Minot, *J. Catal.*, 2006, **241**, 115.
37 Z. P. Liu and P. Hu, *J. Am. Chem. Soc.*, 2003, **125**, 1958.
38 J. Andersin, N. Lopez and K. Honkala, *J. Phys. Chem. C*, 2009, **113**, 8278.
39 L. V. Moskaleva, Z. X. Chen, H. A. Aleksandrov, A. B. Mohammed, Q. Sun and N. Rosch, *J. Phys. Chem. C*, 2009, **113**, 2512.
40 Y. A. Zhu, Y. C. Dai, D. Chen and W. K. Yuan, *J. Mol. Catal. A: Chem.*, 2007, **264**, 299.
41 A. V. Zeigarnik, R. E. Valdés-Pérez and O. N. Myatkovskaya, *J. Phys. Chem. B*, 2000, **104**, 10578.

42 A. V. Zeigarnik and O. N. Myatkovskaya, *Kinet. Catal.*, 2001, **42**, 418.
43 R. T. Vang, K. Honkala, S. Dahl, E. K. Vestergaard, J. Schnadt, E. Laegsgaard, B. S. Clausen, J. K. Nørskov and F. Besenbacher, *Surf. Sci.*, 2006, **600**, 66.
44 A. Binder, M. Seipenbusch, M. Muhler and G. Kasper, *J. Catal.*, 2009, **268**, 150.
45 G. Kresse and J. Hafner, *Phys. Rev. B: Condens. Matter*, 1993, **48**, 13115.
46 G. Kresse and J. Furthmuller, *Comput. Mater. Sci.*, 1996, **6**, 15.
47 G. Kresse and J. Furthmuller, *Phys. Rev. B: Condens. Matter*, 1996, **54**, 11169.
48 J. P. Perdew, K. Burke and M. Ernzerhof, *Phys. Rev. B*, 1996, **77**, 3865.
49 P. E. Blöchl, *Phys. Rev. B: Condens. Matter*, 1994, **50**, 17953.
50 M. Methfessel and A. T. Paxton, *Phys. Rev. B*, 1989, **40**, 3616.
51 G. Henkelman and H. Jonsson, *J. Chem. Phys.*, 1999, **111**, 7010.
52 G. Henkelman and H. Jonsson, *J. Chem. Phys.*, 2001, **115**, 9657.
53 R. A. Olsen, G. J. Kroes, G. Henkelman, A. Arnaldsson and H. Jonsson, *J. Chem. Phys.*, 2004, **121**, 9776.
54 A. Valcárcel, A. Gil, J. M. Ricart and A. Clotet, *Chem. Phys. Lett.*, 2004, **399**, 295.
55 A. T. Anghel, D. J. Wales, S. J. Jenkins and D. A. King, *J. Chem. Phys.*, 2007, **126**, 044710.
56 A. T. Anghel, D. J. Wales, S. J. Jenkins and D. A. King, *Chem. Phys. Lett.*, 2005, **413**, 289.
57 Y. Chen and D. G. Vlachos, *J. Phys. Chem. C*, 2010, **114**, 4973.
58 J. J. W. Harris, V. Fiorin, C. T. Campbell and D. A. King, *J. Phys. Chem. B*, 2005, **109**, 4069.
59 T. Jacob and W. A. Goddard, *J. Phys. Chem. B*, 2005, **109**, 297.
60 A. Stuck, C. E. Wartnaby, Y. Y. Yeo and D. A. King, *Phys. Rev. Lett.*, 1995, **74**, 578.
61 M. L. Yang, Y. A. Zhu, C. Fan, Z. J. Sui, D. Chen and X. G. Zhou, *J. Mol. Catal. A: Chem.*, 2010, **321**, 42.
62 L. J. Song and L. V. C. Rees, *Micropor. Mesopor. Mater.*, 2000, **41**, 193.
63 T. Bligaard, J. K. Nørskov, S. Dahl, J. Matthiesen, C. H. Christensen and J. Sehested, *J. Catal.*, 2004, **224**, 206.
64 R. Alcala, M. Mavrikakis and J. A. Dumesic, *J. Catal.*, 2003, **218**, 178.
65 H. F. Wang and Z. P. Liu, *J. Am. Chem. Soc.*, 2008, **130**, 10996.
66 R. M. Rioux, H. Song, J. D. Hoefelmeyer, P. Yang and G. A. Somorjai, *J. Phys. Chem. B*, 2005, **109**, 2192.
67 P. Forzatti and L. Lietti, *Catal. Today*, 1999, **52**, 165.
68 M. Larsson, M. Hulten, E. A. Blekkan and B. Andersson, *J. Catal.*, 1996, **164**, 44.
69 O. A. Bariås, A. Holmen, E. A. Blekkan, B. Delmon and G. F. Froment, *Stud. Surf. Sci. Catal.*, 1994, 519.
70 F. Abild-Pedersen, J. Greeley and J. K. Nørskov, *Catal. Lett.*, 2005, **105**, 9.

This journal is © the Owner Societies 2011

Phys. Chem. Chem. Phys., 2011, **13**, 3257–3267 | 3267